

Domain Decomposition Coupling of FV4 and DDFV for Numerical Weather Prediction

Oliver Fuhrer, Martin J. Gander, and Sandie Moody

1 Introduction

In the context of Numerical Weather Prediction (NWP) and more precisely in the context of regional weather prediction models, the spatial domains considered usually are non-convex, because of the orography representing mountain ranges. Moreover, the grids used are highly constrained: mesh cells for solving the prognostic equations numerically are much longer and larger than high, e.g. $1.1\text{km} \times 1.1\text{km} \times 10\text{m}$ in COSMO-1. A common practice in NWP is to use terrain-following grids defined such that the distance between the levels grows with altitude (see Figure 1 left). Most weather prediction models use a coordinate change in order to solve the modified prediction equations in a computational domain which uses an equidistant grid (see Figure 1 middle and right). This has the advantage that simple numerical methods such as the finite difference method can be used. However, this also leads to metric terms in the equations due to the mapping, which can cause numerical difficulties.

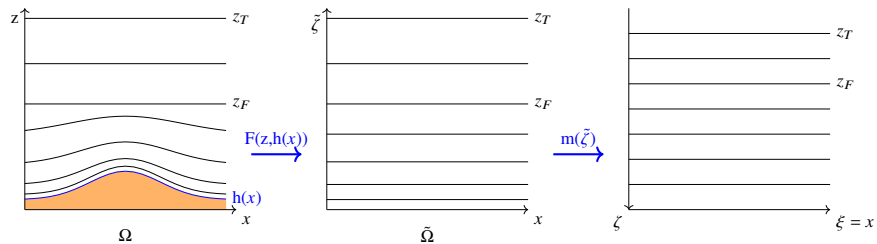


Fig. 1: Mapping of an irregular terrain-following grid to a regular equidistant grid.

Oliver Fuhrer
Vulcan Inc. E-mail: oliverf@vulcan.com

Martin J. Gander and Sandie Moody
Université de Genève. E-mail: {Martin.Gander, Sandie.Moody}@unige.ch

In a terrain-following coordinate system, the lowest surface of constant vertical coordinate is conformal to the orography. Any monotonic function can then be used to define the vertical coordinate, denoted by ζ . The COSMO local model [1] offers three options for the terrain-following coordinate. The first one is a pressure-based vertical coordinate, the second one is a height based coordinate, and the third one is a height based SLEVE (Smooth Level Vertical) coordinate. Both height based coordinates are similar to the *Gal-Chen* coordinate [3]. Figure 1 illustrates the height based hybrid coordinate and its mapping to a regular grid.

Definition 1 Let $h(x)$ denote the height of the local topography. The height based hybrid coordinate is defined by

$$\tilde{\zeta} = \begin{cases} \frac{z - h(x)}{1 - \frac{h(x)}{z_F}} & \text{if } z < z_F, \\ z & \text{if } z_F \leq z \leq z_T, \end{cases}$$

where z_T is the model top.

Numerical weather prediction models are based on a set of seven governing equations. They comprise the equations of motion, the thermodynamic equation, the continuity equation, the equation of state and the water vapour equation. These equations contain diffusion and advection terms which are treated, in the COSMO model, using a time-splitting method. The diffusion is treated implicitly which implies the solution of a Poisson equation of the form

$$\Delta\phi = f, \quad (1)$$

where ϕ can represent wind components, temperature or pressure.

In order to solve a Poisson equation (1) on the original irregular terrain-following grid Ω , the coordinate transformation described above mapping Ω to a regular equidistant grid is used (see Figure 1). The new coordinates are denoted by (ξ, ζ) and we need to compute the transformed Laplace operator in the new coordinate system $(\tilde{\Delta}_{(\xi, \zeta)})$. The derivatives of the new coordinates with respect to the original ones are expressed using subscripts and are called the *metric terms* of the coordinate change.

Proposition 1 Let F be a mapping from $\Omega_{(x,z)}$ to $\tilde{\Omega}_{(\xi, \zeta)}$. Let $u = u(x, z)$ be a function defined on Ω and $F(u) = \tilde{u}(\xi, \zeta)$ be a function defined on $\tilde{\Omega}$. The transformed Laplace operator on $\tilde{\Omega}$ when $\xi(x, z) = x$ is given by

$$\tilde{\Delta}\tilde{u} = \frac{\partial^2 \tilde{u}}{\partial \xi^2} + 2\zeta_x \frac{\partial^2 \tilde{u}}{\partial \xi \partial \zeta} + \frac{\partial^2 \tilde{u}}{\partial \zeta^2} (\zeta_x^2 + \zeta_z^2) + \frac{\partial \tilde{u}}{\partial \zeta} (\zeta_{xx} + \zeta_{zz}). \quad (2)$$

The normal derivative on $\partial\Omega$ is expressed by

$$\frac{\partial u}{\partial \mathbf{n}} = \mathbf{n}^T \begin{pmatrix} \xi_x & \zeta_x \\ \xi_z & \zeta_z \end{pmatrix} \begin{pmatrix} \frac{\partial \tilde{u}}{\partial \xi} \\ \frac{\partial \tilde{u}}{\partial \zeta} \end{pmatrix} = F(\phi) = \tilde{\phi}(\xi, \zeta). \quad (3)$$

Proof Using the chain rule, we find that the second order derivatives on Ω can be expressed by derivatives taken in $\tilde{\Omega}$ by

$$\begin{aligned}\frac{\partial^2 u}{\partial x^2} &= \frac{\partial^2 \tilde{u}}{\partial \xi^2} \xi_x^2 + 2 \frac{\partial^2 \tilde{u}}{\partial \xi \partial \zeta} \xi_x \zeta_x + \frac{\partial^2 \tilde{u}}{\partial \zeta^2} \zeta_x^2 + \frac{\partial \tilde{u}}{\partial \xi} \xi_{xx} + \frac{\partial \tilde{u}}{\partial \zeta} \zeta_{xx}, \\ \frac{\partial^2 u}{\partial z^2} &= \frac{\partial^2 \tilde{u}}{\partial \zeta^2} \xi_z^2 + 2 \frac{\partial^2 \tilde{u}}{\partial \xi \partial \zeta} \xi_z \zeta_z + \frac{\partial^2 \tilde{u}}{\partial \zeta^2} \zeta_z^2 + \frac{\partial \tilde{u}}{\partial \xi} \xi_{zz} + \frac{\partial \tilde{u}}{\partial \zeta} \zeta_{zz}.\end{aligned}$$

Since $\xi = x$, we have $\xi_x = 1$, $\xi_{xx} = \xi_z = \xi_{zz} = 0$ so the second order derivatives reduce to

$$\frac{\partial^2 u}{\partial x^2} = \frac{\partial^2 \tilde{u}}{\partial \xi^2} + 2 \frac{\partial^2 \tilde{u}}{\partial \xi \partial \zeta} \zeta_x + \frac{\partial^2 \tilde{u}}{\partial \zeta^2} \zeta_x^2 + \frac{\partial \tilde{u}}{\partial \zeta} \zeta_{xx}, \quad \frac{\partial^2 u}{\partial z^2} = \frac{\partial^2 \tilde{u}}{\partial \zeta^2} \zeta_z^2 + \frac{\partial \tilde{u}}{\partial \zeta} \zeta_{zz}, \quad (4)$$

which when summed give equation (2). In order to prove (3), we simply need to write the gradient using the chain rule which leads to

$$\mathbf{n}^T \nabla_{(x,z)} u = \mathbf{n}^T \begin{pmatrix} \frac{\partial \tilde{u}}{\partial \xi} \xi_x + \frac{\partial \tilde{u}}{\partial \zeta} \zeta_x \\ \frac{\partial \tilde{u}}{\partial \xi} \xi_z + \frac{\partial \tilde{u}}{\partial \zeta} \zeta_z \end{pmatrix} = \mathbf{n}^T \begin{pmatrix} \xi_x & \zeta_x \\ \xi_z & \zeta_z \end{pmatrix} \begin{pmatrix} \frac{\partial \tilde{u}}{\partial \xi} \\ \frac{\partial \tilde{u}}{\partial \zeta} \end{pmatrix} = \tilde{\phi}(\xi, \zeta). \quad (5)$$

The first disadvantage of this method is that the metric terms ζ_x , ζ_{xx} , ζ_z and ζ_{zz} have to be approximated which leads to instabilities when the mesh size of the grid is very small in the vertical direction in comparison with the horizontal direction, which is typically the case in numerical weather prediction, as we have seen. Moreover, when it is used to solve a time-dependent problem, its CFL condition is quite restrictive. The second disadvantage is that the topography in weather prediction models is represented by the grid as a polygon in contrast to the smooth drawing in Fig. 1 (left). This has as an effect that the first and higher order derivatives of the solution expressed in the new set of coordinates (2) lack continuity in general and so the convergence of the scheme is hampered, as we will see in Section 3. We propose a new method to solve the diffusion equation on such domains and grids; the Discrete Duality Finite Volume (DDFV) method.

2 Discrete Duality Finite Volume Method

The DDFV method was introduced by K. Domelevo and P. Omnes in 2005 (see [2]). F. Hermeline introduced a finite volume method in 2000 which turned out to be equivalent but the construction had less inherent properties (see [6]). DDFV has the advantage that it is adapted to almost arbitrary meshes and geometries.

We now give the notations which we use to define the DDFV method and which are exemplified in Figure 2. The *primal mesh* forms a partition of Ω and is composed of I elements T_i . With each element T_i we associate a *primal node* G_i located inside T_i . The function θ_i^T is the *characteristic function* of the cell T_i . We denote by J the total

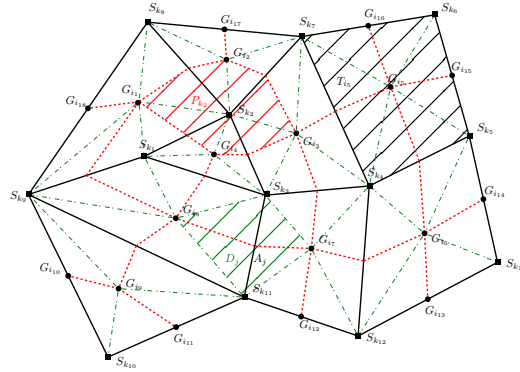


Fig. 2: Notations for the DDFV method.

number of sides of the primal mesh, and by J^Γ the number of these sides which are located on the boundary. We denote the *sides of the primal mesh* by A_j , and assume that they are ordered so that $A_j \subset \Gamma \Leftrightarrow j \in \{J - J^\Gamma + 1, J\}$. We introduce additional primal nodes to each boundary A_j , denoted by G_i with $i \in \{I + 1, \dots, I + J^\Gamma\}$. The nodes of the primal mesh, the *dual nodes* are denoted by S_k with $k \in \{1, \dots, K\}$. To each S_k , we associate a *dual cell* P_k obtained by joining the points G_i associated with the elements of the primal mesh of which S_k is a node. The dual mesh also forms a partition of Ω and its sides are denoted by A'_j . We assume that $S_k \in \Gamma$ if and only if $k \in \{K - J^\Gamma + 1, \dots, K\}$.

To each A_j we associate a *diamond-cell* obtained by joining the nodes of A_j with the primal nodes associated with the primal cells which share the side A_j (see Figure 2). The unit vector normal to A_j is denoted by \mathbf{n}_j and is oriented such that $\langle G_{i_2(j)} - G_{i_1(j)}, \mathbf{n}_j \rangle \geq 0$. Similarly, the unit vector normal to A'_j is denoted by \mathbf{n}'_j and is oriented so that $\langle S_{k_2(j)} - S_{k_1(j)}, \mathbf{n}'_j \rangle \geq 0$. For all $i \in \{1, \dots, I\}$, $j \in \mathcal{V}(i)$ (resp. $k \in \{1, \dots, K\}$, $j \in \mathcal{E}(k)$) we define s_{ji} (resp. s'_{jk}) to be 1 if \mathbf{n}_j points outward of T_i and -1 otherwise (resp. 1 if \mathbf{n}'_j points outward of P_k and -1 otherwise). We thus can define the *outward pointing unit normal vectors* $\mathbf{n}_{ji} = s_{ji}\mathbf{n}_j$ and $\mathbf{n}'_{jk} = s'_{jk}\mathbf{n}'_j$. We define $\mathcal{V}(i) := \{j \in \{1, \dots, J\} \mid A_j \subset T_i\}$ and $\mathcal{E}(k) := \{j \in \{1, \dots, J\} \mid S_k \in A_j\}$.

Definition 2 Let ϕ be defined on Ω . The *discrete gradient* is defined on each diamond-cell by

$$(\nabla_h \phi)_j = \frac{1}{2|D_j|} \left((\phi_{k_2}^P - \phi_{k_1}^P) |A'_j| \mathbf{n}'_j + (\phi_{i_2}^T - \phi_{i_1}^T) |A_j| \mathbf{n}_j \right)$$

where $\phi_{i_\gamma}^T = \phi(G_{i_\gamma})$ and $\phi_{k_\gamma}^P = \phi(S_{k_\gamma})$ for $\gamma \in \{1, 2\}$.

Definition 3 The *discrete divergence* $\nabla_h \cdot$ is defined by its values over the primal and dual cells

$$\begin{aligned}
(\nabla_h \cdot \phi)_i &= \frac{1}{|T_i|} \sum_{j \in \mathcal{V}(i)} |A_j| \phi_j \cdot \mathbf{n}_{ji}, \\
(\nabla_h \cdot \phi)_k &= \frac{1}{|P_k|} \left(\sum_{j \in \mathcal{E}(j)} |A'_j| \phi_j \cdot \mathbf{n}'_{jk} + \sum_{j \in \mathcal{E}(j) \cap \{J-J^\Gamma+1, \dots, J\}} \frac{1}{2} |A_j| \phi_j \cdot \mathbf{n}_j \right).
\end{aligned}$$

Let us consider the Poisson equation (1) with homogeneous Dirichlet boundary conditions. We use the discrete DDFV divergence and gradient operators defined above to approximate the Laplacian which leads to the scheme

$$\begin{cases}
-(\nabla_h^T \cdot (\nabla_h \phi))_i = f_i^T & \forall i \in \{1, \dots, I\} \\
-(\nabla_h^P \cdot (\nabla_h \phi))_k = f_k^P & \forall k \in \{1, \dots, K - J^\Gamma\} \\
\phi_i^T = 0 & \forall i \in \{I+1, \dots, I+J^\Gamma\}, \\
\phi_k^P = 0 & \forall k \in \{K - J^\Gamma + 1, \dots, K\},
\end{cases} \quad (6)$$

where

$$f_i^T = \frac{1}{|T_i|} \int_{T_i} f(x) dx, \quad f_k^P = \frac{1}{|P_k|} \int_{P_k} f(x) dx.$$

Proposition 2 ([2], Proposition 3.2.) *The linear system given by (6) possesses a unique solution in V where V is defined by*

$$\begin{aligned}
V := \left\{ \phi = ((\phi_i^T), (\phi_k^P)) \in \mathbb{R}^{I+J^\Gamma} \times \mathbb{R}^K \mid \phi_i^T = 0 \forall i \in \{I+1, \dots, I+J^\Gamma\} \right. \\
\left. \text{and } \phi_k^P = 0 \forall k \in \{K - J^\Gamma + 1, \dots, K\} \right\}.
\end{aligned}$$

3 Coupling of DDFV and FV4

One of the main concerns of weather prediction services is computational costs. Due to the fact that the DDFV method introduces additional nodes, the size of the linear system which has to be solved is roughly twice as large as the one associated with the classical Finite Volume (FV4) method. A coupling of FV4 and DDFV allows to reduce the size of this linear system considerably. Such a coupling could be achieved using optimized Schwarz techniques, see for example [7, 5, 4], but we propose here a different approach using interpolation. Let us consider a rectangular domain Ω which has a mountain at its center with slope α , see Figure 3. All cells which are not directly above the mountain are rectangular, so the standard FV4 scheme can be applied on those cells. To the cells which are irregular quadrilaterals, we apply the DDFV method (see Figure 3, left). The points at the interface (“black diamonds”) are dual points which were needed for the DDFV equations associated with primal points (“white squares”) and the dual points (“black squares”) at the interface. However, they are not associated with a dual cell (see Figure 3, right), so we need to define

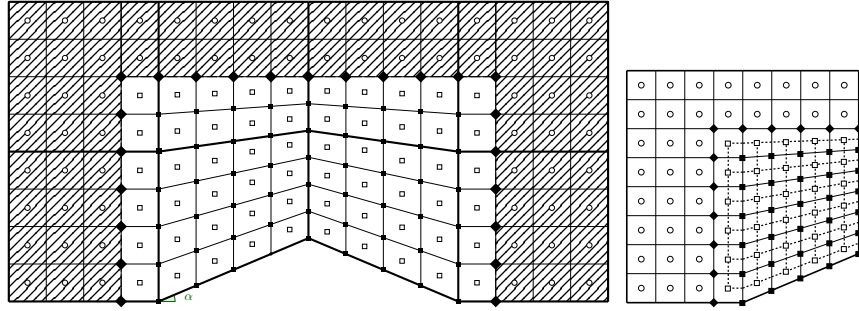


Fig. 3: (Left) Hatched area: Finite volume. White area: DDFV. (Right) FV4 point, primal DDFV points, dual DDFV points and interface points.

a coupling equation. An intuitive way to define the coupling is to set the value of the interface dual points to be the weighted average of its four primal neighboring points, which defines our DDFV-FV4 coupled scheme. For testing purposes, let us consider the problem

$$\Delta u = -5\pi^2 \sin(2\pi x) \sin(\pi y) \text{ on } \Omega,$$

with Dirichlet boundary conditions on the left and right of the domain and Neumann boundary conditions at the top and the bottom of the domain. The order of convergence of both the DDFV method and the DDFV-FV4 coupled method for this problem is 2 (see Figure 4). As for the error, which we define to be the infinity-norm of the difference between the exact solution and the numerical solution, it has a stronger dependence on the mountain angle α for the DDFV method. We then compare the time in seconds needed to solve the linear system associated with the coupled scheme and the DDFV scheme alone. We consider different domains which induce different percentages of the domain to be covered by the DDFV method i.e. different percentages of cells which are not rectangular (column “DDFV-FV4” in

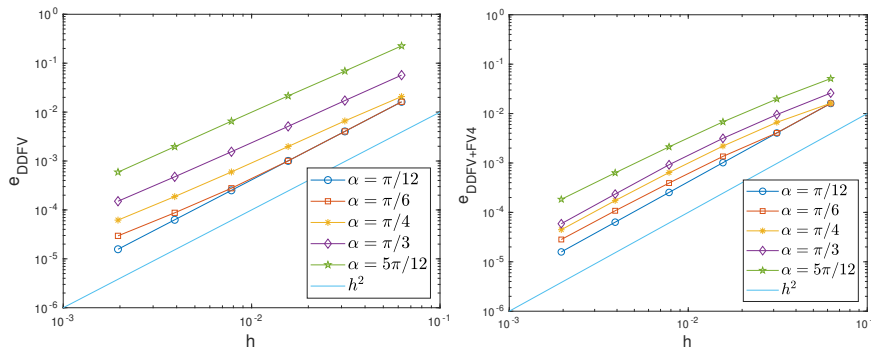


Fig. 4: Error of the DDFV method on the left and error of the DDFV-FV4 coupled scheme on the right.

DDFV-FV4				COSMO			
	n	time in sec.	error		n	time in sec.	error
14%	128	0.092837	0.0035973	14%	128	0.07799	0.038027
	256	0.47006	0.0010113		256	0.42181	0.022181
18%	128	0.10192	0.0036404	18%	128	0.083277	0.037821
	256	0.58811	0.0010218		256	0.43485	0.021982
37%	128	0.13081	0.004225	37%	128	0.088778	0.10018
	256	0.73254	0.00111		256	0.50752	0.048907
56%	128	0.20006	0.0038666	56%	128	0.10705	0.085701
	256	1.0613	0.00096342		256	0.53349	0.051025
79%	128	0.23772	0.0048132	79%	128	0.12153	0.12076
	256	1.1817	0.0012051		256	0.60488	0.05706
79% DDFV	128	0.19662	0.0044965				
	256	0.98724	0.0011279				

Table 1: Computational time and error of the DDFV-FV4 coupled scheme.

Table 1). We also compute the time and error obtained when using the scheme based on the coordinate transformation described in Section 1 (column “COSMO” in Table 1). We see that the coupled scheme leads to excellent accuracy, even when only a small percentage of DDFV is needed. We note however that even though the coupling method has less degrees of freedom, it is not always faster than the DDFV method. This is due to the fact that our linear system associated with the coupled method is non-symmetric, see Figure 5, whereas the DDFV method gives a symmetric matrix, which is inverted more efficiently by the Matlab solver we use.

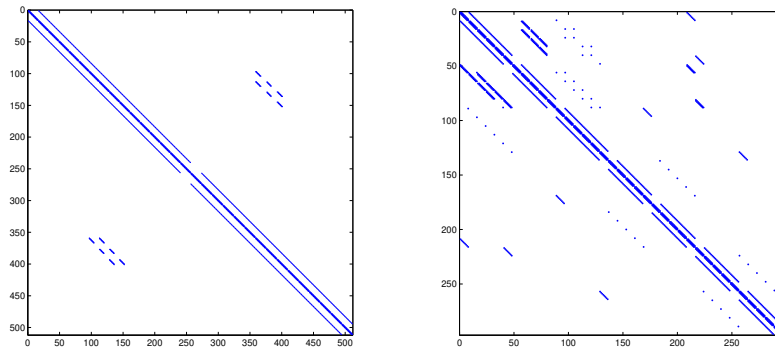


Fig. 5: Structure of the linear system associated to the DDFV method (left) and DDFV-FV4 method (right).

4 Conclusion

We presented a DDFV scheme which does not need a mapping to a regular grid on a rectangular domain for a faithful discretization of diffusion operators on the high aspect ratio grids typical in numerical weather prediction. Moreover, the scheme presented converges on domains which lead to discontinuities in the derivatives of the solution when a mapping to a regular grid is used. Since DDFV uses twice as many unknowns than a standard FV4, we also introduced a coupled DDFV-FV4 scheme which only uses DDFV where it is needed due to the mountain orography. We observed second order convergence for both DDFV and DDFV-FV4. When measuring computing times, the coupled scheme is only faster when less than half the domain is treated by DDFV, even though it always has less unknowns than the DDFV method. We identified the reason for this to be the non-symmetry introduced by our coupling through interpolation between DDFV and FV4. It is currently an open question if a symmetric coupling of these two schemes is possible.

References

1. COSMO-model Documentation. <http://www.cosmo-model.org/content/model/documentation/core/default.htm> (2019). [Online; accessed 11-March-2019]
2. Domelevo, K., Omnes, P.: A Finite Volume Method for the Laplace Equation on Almost Arbitrary Two-dimensional Grids. *ESAIM: Mathematical Modelling and Numerical Analysis* **39**(06), 1203–1249 (2005)
3. Gal-Chen, T., Somerville, R.C.J.: On the Use of a Coordinate Transformation for the Solution of the Navier-Stokes Equations. *J. Comput. Phys.* **17**, 209–228 (1975). DOI: [10.1016/0021-9991\(75\)90037-6](https://doi.org/10.1016/0021-9991(75)90037-6)
4. Gander, M.J., Halpern, L., Hubert, F., Krell, S.: DDFV Ventcell Schwarz algorithms. In: *Domain Decomposition Methods in Science and Engineering XXII*, pp. 481–489. Springer (2016)
5. Gander, M.J., Hubert, F., Krell, S.: Optimized Schwarz algorithms in the framework of DDFV schemes. In: *Domain Decomposition Methods in Science and Engineering XXI*, pp. 457–466. Springer (2014)
6. Hermeline, F.: A Finite Volume Method for the Approximation of Diffusion Operators on Distorted Meshes. *Journal of Computational Physics* **160**(2), 481 – 499 (2000). DOI: <https://doi.org/10.1006/jcph.2000.6466>. URL <http://www.sciencedirect.com/science/article/pii/S0021999100964660>
7. Krell, S.: Finite Volume Schemes for Complex Fluid Mechanics. Thèse, Université de Provence - Aix-Marseille I (2010). URL <https://tel.archives-ouvertes.fr/tel-00524509>